Toroidal modelling of plasma response and RMP field penetration

Y.Q. Liu[1], A. Kirk[1], Y. Sun[2], Y. Gribov[3], M.P. Gryaznevich[1], T.C. Hender[1], E. Nardon[4]
[1]*Euratom/CCFE Fusion Association, Culham Science Centre, Abingdon, OX14 3DB, UK*
[2] *EURATOM/FZJ Fusion Association, Trilateral Euregio Cluster, 52425 Jülich, Germany*
[3]*ITER Organization, Route de Vinon sur Verdon, 13115 St Paul Lez Durance, France*
[4]*Euratom/CEA Fusion Association, 13108 St Paul-lez-Durance, France*

1. Introduction.

It is expected that large scale, low frequency type-I edge localised modes (ELMs) may not be tolerable for the plasma facing components in ITER, due to the large heat load. Extensive experimental results from recent years, on several existing tokamak devices, have demonstrated that the externally applied resonant magnetic perturbation (RMP) fields can significantly affect the behaviour of ELMs. It appears that the ELM mitigation/suppression, and the accompanying density pump-out effect observed in experiments, require detailed investigations due to complex physics. An important role is played by the plasma response to the RMP fields. This has at least two aspects: (i) the plasma response changes the vacuum field spectrum, especially near the rational surfaces. Consequently, the magnetic field line ergodisation, believed to be responsible for the enhanced transport near the plasma edge and partial flattening of the pedestal pressure profile, depends crucially on the plasma response; (ii) the RMP fields, together with the plasma response, can induce a toroidal torque on the plasma, resulting in toroidal momentum damping. Since the plasma flow itself provides a screening effect on the RMP field penetration, the whole penetration process forms a feedback loop, when the plasma response is included.

In this work, we present numerical results of the linear plasma response to the RMP fields, as well as quasi-linear field penetration and momentum damping, using the linear MHD code MARS-F [1] and an updated version of the code, the quasi-linear version MARS-Q. The modelling is performed for realistic plasmas in full toroidal geometry.

2. Linear plasma response to RMP fields.

We consider a resistive, single fluid plasma model, with arbitrary toroidal flow and flow shear [2]. Detailed plasma response computations have been performed for both MAST and ITER plasmas [3]. We find that the resistive plasma response in general substantially reduces the total field near rational surfaces for resonant RMP harmonics, but also yields a mild amplification of the non-resonant components, in the plasma regimes considered for ELM mitigation. The plasma response, however, is a sensitive function of the plasma toroidal rotation speed (i.e. the screening effect). Moreover, we also numerically find a correlation between the computed plasma surface displacement, more precisely the poloidal distribution of the normal displacement, and the observed density pump-out in the experiments on MAST.

As one example, figure 1(a) compares the computed amplitude of the surface displacement along the poloidal angle for the two coil parities, for one of the MAST L-mode plasmas. In the even (odd) parity configurations, the current in the upper and lower sets of the MAST ELM control coils flow in the same (opposite) direction. The even parity configuration in this case causes a large distortion of the plasma surface near the X-points, in correlation with the density pump-out effect observed in the MAST experiment.

Further investigation reveals that different coil parities can cause different dominant mode re-

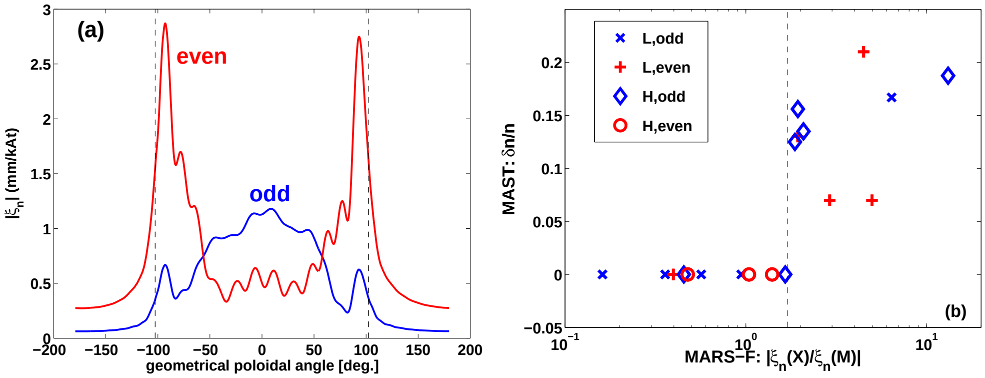

Figure 1: *(a) Comparison of the MARS-F computed normal displacements of the plasma surface with odd versus even parities of the RMP coil current, for shot 25056. The dashed vertical lines indicates the poloidal location of the X-points. (b) Correlation between the computed normal displacement of the plasma surface, and the observed density pump-out effect in all types of MAST plasmas from the RMP experiments. Plotted is the experimental density pump-out fraction versus the ratio of the displacement peaking near the X-point ($\xi_n(X)$) to that at the outboard mid-plane ($\xi_n(M)$).*

sponses from a stable plasma. For the case shown in Fig. 1(a), the odd parity coils cause a predominantly kink mode response, whilst the even parity coils cause a predominantly peeling-tearing like mode response. The poloidal distribution of the plasma surface displacement (the X-point peaking versus the outboard mid-plane peaking) is robustly correlated with different types of the plasma response caused by the magnetic perturbation coils.

Our additional modelling covers all types of MAST plasmas from the RMP experiments so far, and we find that the ratio of the displacement peaking near the X-points, to that at the outboard mid-plane, seems to be the best indicator for the observed density pump-out effect. Shown in Fig. 1(b) is the experimental observation (the fraction of pumped out density) versus the MARS-F computed displacement peaking ratio. For all cases, the measured toroidal plasma rotation from experiments was used in the modelling. The vertical dashed line, separating the two cases, is at $|\xi_n(\mathrm{X})/\xi_n(\mathrm{M})| = 1.7$. This indicator works well for all types of L-mode and H-mode plasma studied so far in experiments. The criterion is less robust for H-mode plasmas, in the sense that there is a very narrow gap in the value of the displacement indicator, crossing the cases without and with the observed density pump-out. No clear physics explanantion is currently available, that couples the density pump-out to the plasma surface displacement, though some speculations can be envisaged [3].

3. Toroidal momentum balance.

We solve a toroidal momentum equation derived from the force balance equation, which includes both the fluid electromagnetic $j \times b$ force and the neoclassical toroidal viscous (NTV) force. The momentum diffusion and pinch operators are also included in the mometum balance equation. The momentum equation is numerically solved using a finite element method (FEM) along the radial grid, with homogeneous Neumann boundary conditions for ΔL, the change of the toroidal momentum due to the RMP field, at both the plasma centre and edge. An analytic test case has been designed to test the momentum solver in MARS-Q.

We consider a toroidal equilibrium described in [2]. The equilibrium current and pressure profiles, as well as the plasma boundary shape is specified analytically for this equilibrium, with the plasma major radius of $R_0 = 3$m, the vacuum toroidal magnetic field B_0=1.5Tesla, and the aspect ratio $R_0/a = 3$. The plasma boundary has an elongation $\kappa = 1.6$ and triangularity

$\delta = 0.3$. The equilibrium current and pressure are chosen to have $q_0 = 1.25, q_{95} = 4.21, q_a = 5.24$, and the normalised pressure $\beta_N = 1.46$, far below the no-wall limit of 3.99 for the $n = 1$ ideal external kink instability. The total plasma current is 1.28MA. For simplicity, we consider a resistive plasma with uniform resistivity along the minor radius. For a default case, we set the magnetic Lundquist number to be $S = 10^6$.

For test computations, we consider the RMP field produced by a set of coils located at $(R,Z) = (4.98,1)$m and $(4.98,-1)$m. These coils are outside a resistive wall located at the minor radius of $1.23a$. As the default case, we choose the coil current equivalent to 24kA-turn, flowing in one pair of opposite coils in the JET-like error field correction coil configuration, producing a predominant $n = 1$ RMP field.

Prescribing a toroidal plasma rotation, the linear response of the plasma to the RMP field can be computed using MARS-F [2]. The plasma response (e.g. the $n = 1$ perturbed current, the magnetic field, and the plasma displacement) can be used to further compute the $n = 0$ toroidal torques, such as the electromagnetic $j \times b$ torque and the NTV torque. The NTV torque is computed here using formulae from Ref. [4], where various regimes (the so-called ν- and $1/\nu$ regimes, as well as the boundary layers) are smoothly connected.

Assuming that the plasma central rotation reaches 3% of the Alfvén speed (with the rotation profile as specified in Ref. [2]), MARS-Q computations show that the NTV torque is generally smaller than the $j \times b$ torque, in the presence of the RMP field. In the plasma core region, the difference reaches two orders of magnitude.

4. Quasi-linear modelling of RMP field penetration.

The MARS-Q code allows quasi-linear simulations of the RMP field penetration dynamics and the plasma toroidal momentum damping, by coupling the $n \neq 0$ perturbed, full MHD equations with the $n = 0$ toroidal momentum balance equation. The modelling is performed for full toroidal geometry. These are the major difference from a previous work [5], based on a four-field reduced MHD model, and the cylindrical geometry.

In order to solve the coupled equations, we adopt a time-stepping strategy, where the MHD operators are all included in a fully implicit scheme. This allows us to take time steps larger than the Alfvén time. The quadratic terms in toroidal torques are time-advanced using an explicit scheme, based on a staggered grid in time. We find that a time step of $\Delta t = 10\tau_A$ can be chosen, without losing the numerical stability and accuracy. We also allow a simple adaptive scheme in time-stepping.

As for physical parameters, we consider a resistive plasma with the magnetic Lundquist number $S = 10^6$ and $S = 10^5$ (with a uniform resistivity profile across the plasma column). These S-values are probably too small to describe the plasma core, but is reasonable for the plasma edge region, which is the region of our primary interest. We choose the anomalous toroidal momentum diffusion coefficient χ_M, normalised by $R_0 v_A$, to be $\chi_M = 3 \times 10^{-7}$ at the plasma centre. This value would correspond to several m^2/s for JET-like plasmas [6]. We choose the radial profile of χ_M as $\propto T_e^{-3/2}$, with T_e being the equilibrium electron temperature. The pinch velocity is neglected. Both the $j \times b$ and NTV torques are included in the momentum equation. We consider a special saturation condition for the toroidal rotation damping, by freezing the rotation frequency to a near-zero value ($10^{-4}\omega_A$), as soon as the total toroidal rotation switches sign.

Our modelling shows that the plasma resistivity sensitively affects the RMP field penetration

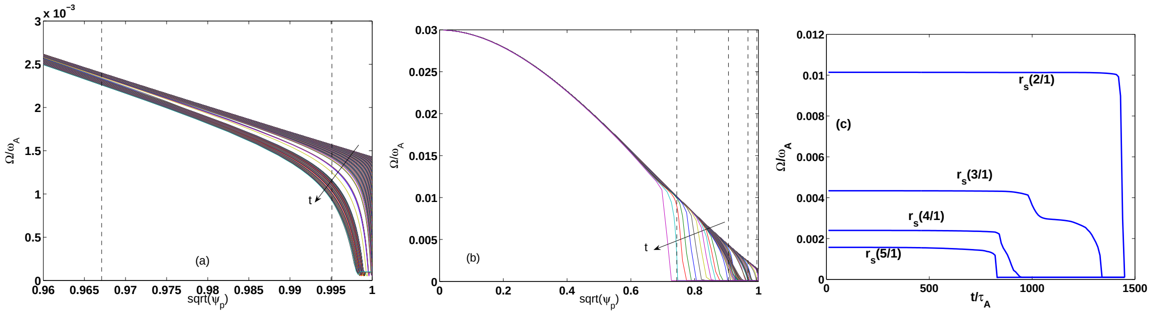

Figure 2: *Effect of the plasma resistivity on the profile evolution of the toroidal rotation frequency: (a) with the magnetic Lundquist number $S = 10^6$, (b) with $S = 10^5$, (c) time evolution of the rotation amplitude at rational surfaces, indicated by vertical dashed lines in (a) and (b), with m/n=2/1,3/1,4/1, and 5/1, respectively, for the case with $S = 10^5$.*

dynamics, and the rotation damping. Figure 2(a-b) compares the evolution of the toroidal rotation profiles, with the magnetic Lundquist number $S = 10^6$ and $S = 10^5$, respectively. We notice that the rotational damping generally propagates from the plasma boundary towards the core region. Higher plasma resistivity leads to faster field penetration and stronger damping of the rotation near the plasma edge. This agrees with qualitative understanding that the magnetic islands penetrate with vanishing plasma rotation at rational surfaces. We also note that the simulation in these studies is terminated at $t = 2000\tau_A$. This corresponds to about 2ms time interval assuming a typical Alfvén time of $\tau_A = 1\mu$s. In order to follow the full penetration dynamics, in particular for the more realistic resistivity case ($S = 10^6$), it is desirable to continue the simulation beyond 2ms in further studies.

The speed of the RMP field penetration and the rotational damping is better measured by plotting the time behaviour of the rotation amplitude at various rational surfaces. One case is shown in Fig. 2(c), for a highly resistive plasma with $S = 10^5$. Note that, due to the saturation condition applied to the toroidal rotation, the time trace remains constant after reaching a near-zero value. Without the saturation condition, the rotation amplitude keeps decreasing with time, and can become negative near the very edge of the plasma.

In order to understand the relative contributions from the $j \times b$ torque and the NTV torque, we also run simulations by switching off one of the torques, and follow the time trace of the rotational damping. We find that the fluid $j \times b$ torque provides a stronger damping to the rotation than the NTV torque, even near the plasma edge region.

Acknowledgements. This work was part-funded by the RCUK Energy Programme under grant EP/I501045 and the European Communities under the contract of Association between EURATOM and CCFE. The views and opinions expressed herein do not necessarily reflect those of the European Commission.

References

[1] Liu Y Q *et al* 2000 *Phys. Plasmas* **7** 3681
[2] Liu Y Q *et al* 2010 *Phys. Plasmas* **17** 122502
[3] Liu Y Q *et al* 2011 *Nucl. Fusion* in press
[4] Shaing K C *et al* 2010 *Nucl. Fusion* **50** 025022
[5] Nardon E *et al* 2010 *Nucl. Fusion* **50** 034002
[6] Sun Y *et al* 2010 *Plasma Phys. Control. Fusion* **52** 105007